

Simulation Analysis of Shell Plate-Type Heat Exchanger Using Liquefied Natural Gas Cold Energy for Refrigerated Warehouses

Danbee Han¹, Youngsoon Baek†², Wooksang Cho³, Jaerin Shin⁴

^{1,2,3}*Department of Environment-Energy, Suwon University of Suwon, Hwaseong-si, Geonggi-do, 18323, Korea*

⁴*EUGENE Super Freeze Co. Institute of Technology, Yongin-si, Geonggi-do, 16827, Korea*

Abstract- When liquefied natural gas (LNG) is vaporized to form natural gas for industrial and household consumption, a significant amount of cold energy is transferred from the LNG to seawater as a part of the phase-change process; this heat exchange loop is not only a waste of cold energy, but causes thermal pollution in coastal fishery areas because of the dumping of cold energy into the sea. Through vaporization of a refrigerant, the cold energy captured by the refrigerant can be used as an energy source in electrically operated refrigeration warehouses. Thus, in this study, simulations were conducted for a shell-plate-type heat exchanger applied to an electric refrigeration warehouse using LNG cold energy with an HTRI simulator. Furthermore, by comparing the simulation results with water-water heat exchanger experimental results, the reliability of our simulations was validated. In addition, by changing the number of plates and spacing between these plates in the simulations, the optimal values for these two variables for the shell-plate-type heat exchanger were obtained.

Keywords – LNG, Cold energy, Shell-plate-type Heat exchanger, Refrigerated Warehouses, Simulation

I. INTRODUCTION

For convenience of transportation from overseas gas fields in Indonesia, Brunei, and Malaysia, among others, to Korea, Natural Gas (NG) is liquefied to form Liquefied Natural Gas (LNG) using low temperature and high pressure conditions after removing nitrogen, carbon dioxide, and other impurities from it using gas treatment equipment. In particular, LNG consists of methane, ethane, propane, and butane, among others.

The storage density of LNG is 625 times higher than that of NG (gas state); in addition, LNG is in the cryogenic liquid state at about -162°C. LNG is imported into South Korea through LNG carriers, where it is unloaded and stored in LNG storage tanks at Incheon, Pyeongtaek, Tongyeong, and Samcheok LNG terminals. To supply this LNG to homes, it is passed through vaporizers; in particular, open rack vaporizers (ORVs), which use sea water at room temperature and submerged combustion vaporizers (SMVs), which use combustion gas, are utilized. However, LNG cold energy of about 830–860 kJ/Kg is lost to the sea or air, totaling about 7.6×10¹² kcal annually, even though LNG usage in South Korea is about 3.8 million ton per year (as of 2016). This wasted cold energy is not only enormous, but also hampers the sea and air ecosystems.

There are about 780 electric refrigeration warehouses currently operating in South Korea; however, this number is steadily increasing, and it is forecasted that the annual cold energy reaching a maximum of 3.3×10¹² kcal will be used for LNG refrigeration warehouses. We expect that the core technology developed in this research will not only replace conventional electric energy used in cold storage warehouses (operating below -100°C), but it will also reduce 50–70% of the operating power costs of these refrigeration warehouses, greatly facilitating the distribution industry [1].

In this study, heat exchangers in LNG refrigeration warehouse systems that replace the electric refrigeration systems and use LNG cold energy, were analyzed using a commercial Heat Transfer Research Institute (HTRI) simulator. Our analysis was performed using the shell-plate-type heat exchanger as the primary heat exchanger, in which the LNG and refrigerant followed counter-current flows; the plate thickness and diameter were 0.4 T and 325 mm, respectively. By comparing the simulation results of the heat exchanger with the experimental data, the reliability of our simulation results was validated. To optimize the LNG shell-plate-type heat exchanger, the effect of the overall heat transfer coefficient (U), effective area (A), and overdesign rate on the efficiency of the heat exchanger were analyzed based on different number of plates and spacing between them.

II. SIMULATIONS AND EXPERIMENTAL STUDY

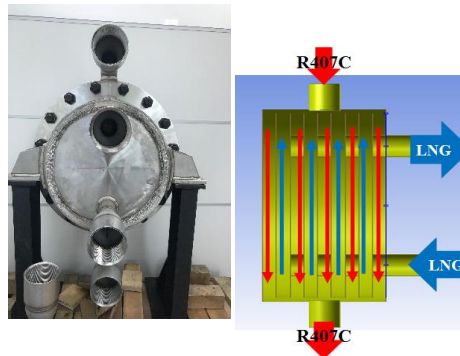
2.1 Structure of shell-plate-type heat exchanger –

As shown in Fig. 1, the shell-plate-type heat exchanger overcomes the limitation of the plate-type heat exchanger, which cannot be operated at high pressure. In the shell-plate-type heat exchanger, several plates are joined together to form one module, and then, based on the required heat exchange rate, several of these modules are combined to construct the appropriate heat exchanger.

Because both fixed and moveable plates are assembled on a guide bar in the case of the plate-type heat exchanger, it has a simple structure; therefore, based on the required capacity, the number of plates can be easily increased or decreased [2]. Although loss in pressure can be controlled using the water channel flow rate of the heat exchanger channel, as previously mentioned, the plate-type heat exchanger is not a suitable heat exchanger for high temperature and high pressure operating conditions.

In contrast, the shell-tube-type heat exchanger can be operated at high temperatures and pressures; furthermore, the shell-plate heat exchanger was developed to overcome the drawbacks of the abovementioned heat exchangers and benefit from their strengths. It has excellent efficiency at both high temperature and pressure as well as low temperature [3]. In particular, the shell-plate heat exchanger has a structure that is based on the multiple-tube-type shell-tube and plate heat exchangers.

As previously indicated, the efficiency of the plate-type heat exchanger is affected by the total number of plates and spacing of plates. In the case of the shell-plate-type heat exchanger, similar to the plate-type heat exchanger, because the conditions of the channels, in which the LNG and refrigerant flow, change depending on the number of plates and spacing between them, it is believed that it affects the efficiency of the heat exchanger. Moreover, because these flows also affect the size of the heat exchanger, it is possible to obtain an optimal configuration for the heat exchanger by modifying these characteristics.



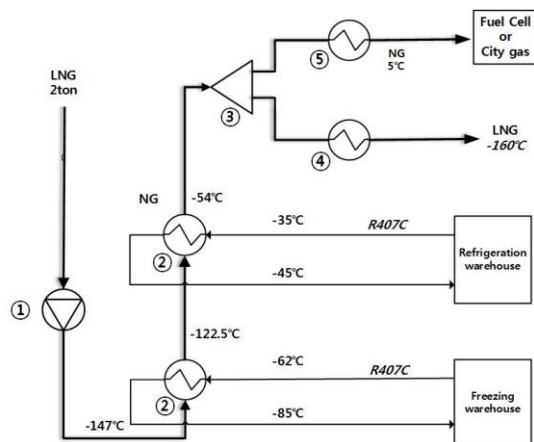
Test product for the shell-plate-type exchanger and flow directions of the LNG and R407C refrigerant.

2.2 Simulation of the shell-plate-type heat exchanger –

Fig. 2 shows the heat exchange process at a refrigeration warehouse using LNG cold energy; in this case, the shell-plate-type heat exchanger is used as the primary heat exchanger.

In the heat exchanger, the two fluids have counter-current flows; in particular, the LNG flows upward from the bottom, whereas the R407C refrigerant flows downward after being injected at the top, exchanging heat with the LNG as they pass through the exchanger. The heat exchanger has 27 plates providing an effective area of 2.04 m², with a 5-mm spacing between plates; the plates are 0.4 T thick and are made from SUS304 material.

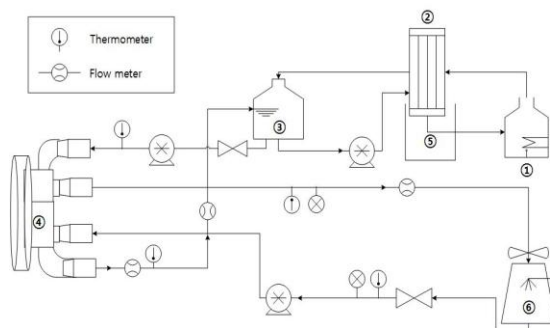
This shell-plate heat exchanger was analyzed via heat exchanger simulation conducted using the HTRI Phe simulator. For this simulation, the type and flow rate of the fluid passing through the heat exchanger as well as the temperature and pressure at its inlet were set to be the same as those of the operating conditions of the heat exchange system when cold energy is used. Based on the simulation, the temperature of the fluid at the outlet and heat exchange rate between the LNG and refrigerant were calculated.



Schematic diagram of a refrigeration warehouse using LNG cold energy: 1. Pump 2. LNG heat exchanger (Primary and secondary HX) 3. Distributor 4. Re-liquefaction 5. Heater

2.3 Experimental apparatus and method –

For our experiments, water-water experiments were conducted instead of LNG-refrigerant heat exchange experiments. The apparatus of the heat exchanger performance experiment was configured as shown in Fig. 3; under atmospheric pressure conditions, water was injected into the heat exchanger and by measuring the temperature of fluid exiting the outlet, the heat exchange rate between the two fluids was measured. In particular, by operating the circulating pump for cooling water, cold water was supplied to the sample and the flow rate change of the cold water was controlled using the opening rate of the ball valves installed at the inlet and outlet pipes of the heat exchanger. Hot water was supplied to the heat exchanger by operating the circulating pump for hot water and the flow rate change of the hot water was controlled via the revolutions-per minute (RPM) speed of the pump motor using an inverter. The temperature of the hot water was adjusted by controlling the electric current supplied to the heating element inserted inside the heater. When the flow rates of hot and cold water stabilized, and the temperature changes in the hot water are maintained in the fluctuation range of less than $\pm 1.0^{\circ}\text{C}$, the fluids are determined to be in a “normal state”.



Schematic diagram of the experimental apparatus. 1. Steam boiler 2. Heat exchanger 3. Water tank 4. Shell-plate heat exchanger 5. Condensed water 6. Cold water basin.

The abovementioned data were acquired for a duration of 100 s when the outlet temperature ($32 \pm 1.0^{\circ}\text{C}$) of the hot and cold fluid (32 ± 1.0) were stable.

Based on the results of the above experiment, the heat exchange rate (Q_h) of the hot liquid as well as the heat exchange rate (Q_c) of the cold liquid at their respective outlets were calculated using Eq. (1) and (2), respectively; then, the average heat exchange rate Q_{avg} was obtained using Eq. (3) [4].

$$Q_h = m \cdot C_p \cdot [T_i - T_o]_h \quad (1)$$

$$Q_c = m \cdot C_p \cdot [T_o - T_i]_c \quad (2)$$

$$Q_{avg} = (Q_h + Q_c) / 2 \quad (3)$$

where m is mass flow rate (m^3/h), C_p is specific heat capacity ($\text{kcal}/\text{kg} \cdot ^{\circ}\text{C}$), T_i ($^{\circ}\text{C}$) is inlet temperature, and T_o ($^{\circ}\text{C}$) is outlet temperature.

Simulation for optimization of the heat exchanger –

The spacing of the plates in the heat exchanger is the width of the channel where the fluid flows; because this spacing affects the overall heat transfer coefficient or pressure of the fluid, it also affects the efficiency of the heat exchange in the exchanger. When the number of plates involved in the heat exchange increases, consequently, the effective area of heat exchange increases; therefore, to obtain the same fluid temperature under the same rate of heat exchange, the overall heat transfer coefficient needs to be decreased.

The overdesign of the heat exchanger indicates the desired efficiency ratio of the heat exchanger that needs to be obtained from the current heat exchanger design when the temperature or heat exchange rate is fixed. Considering this, the design factors can be modified to obtain the desired heat exchange [5].

Thus, the shell-plate heat exchanger can have variable number of plates and spacing between the plates. In our study, the values of effective area (A) and overall heat transfer coefficient (U) for the heat exchanger were analyzed by changing the number of plates and spacing between the plates for optimization.

III. RESULTS AND DISCUSSION

3.1 Heat exchanger simulation results –

For the refrigeration warehouse using LNG cold energy, as previously mentioned, the analysis conditions of the shell-plate heat exchanger were as follows: 27 plates (26 channels) with a 5-mm plate spacing and 0.4 T plate thickness yielding an effective area of 2.04 m². The simulation results are listed in Table 5; as can be seen from the Table, the outlet temperature of LNG at -121.5°C and outlet temperature of R407C at -85°C were considerably similar to the values of the processing conditions of system.

Table -1 Simulation result of the shell-plate-type heat exchanger for the LNG-R407C system using the HTRI simulator

Unit	LNG	R407C
Mass flow (kg/h)	2,000	13,530
Temp. (°C)	IN	-147
	OUT	-62
Temp. (°C)	IN	-121.5
	OUT	-85
Q (kcal/h)	92,700	

3.2 Heat exchanger experiment and simulation validation –

Table 2 lists the results of the water-water experiment conducted at atmospheric pressure conditions with a system configuration as shown in Fig. 3.

The respective heat exchange rates of the fluids flowing on the hot and cold sides of the heat exchanger were obtained using Eqs. (1) and (2); in particular, for Sample #1–3, the heat exchange rates of the hot side were 33,300, 34,858, and 35,100 kcal/h, respectively, while those for the cold side were 25,300, 30,792, and 30,700 kcal/h, respectively. For each sample, the average heat exchange rate of the two fluids Q_{avg} was 29,000, 32,825, and 32,400 kcal/h, respectively. At the inlet and outlet of the shell-plate heat exchanger, there was almost no pressure drop and atmospheric pressure was maintained.

Table -2 Experimental result of shell-plate-type heat exchanger

Sample		Mass flow (m ³ /h)	Temp. (°C)		Q (kcal/h)	Q _{avg} (kcal/h)
			In	Out		
#1	Hot	10.09	34.93	31.62	33,324	29,334
	Cold	4.32	25.87	31.74	25,345	
#2	Hot	9.97	35.16	31.66	34,858	32,825
	Cold	4.32	24.69	31.82	30,792	
#3	Hot	10.06	35.40	31.91	35,100	32,400
	Cold	4.33	25.20	32.07	29,699	

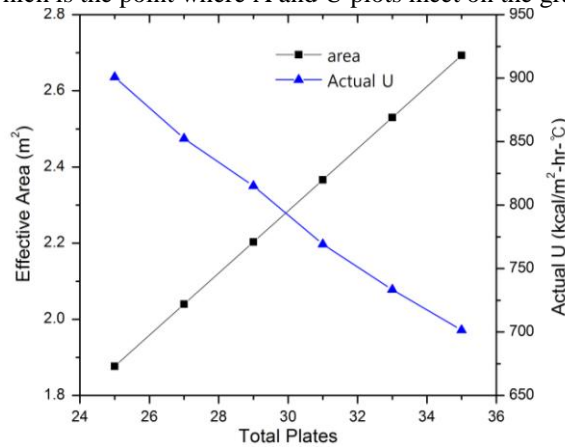
Furthermore, as listed in Table 3, the results of the simulation with the same conditions as in Experiment #1 yielded the heat exchange rates for the hot (Q_h) and cold (Q_c) fluids as 33,300 kcal/h and 25,200 kcal/h, respectively, with an average heat exchange rate (Q_{avg}) of 29,250 kcal/h, values which are similar to the values obtained from the experiment. Therefore, the simulation results can be considered as reliable.

Table -3 Simulation results of the shell-plate heat exchanger for the water-water setup using the HTRI simulator

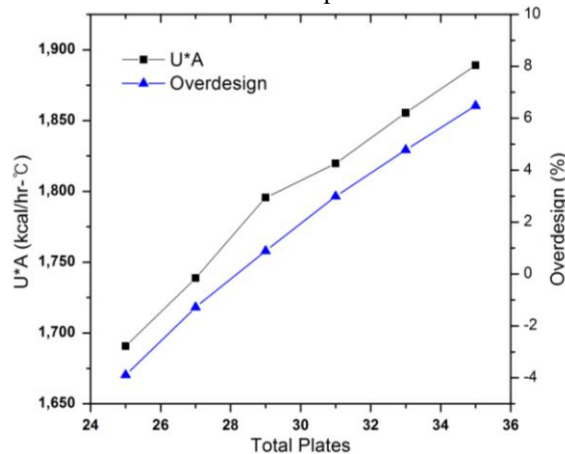
Unit		HTRI (hot)		HTRI (cold)	
		Hot water	Cold Water	Hot water	Cold Water
Mass flow (kg/h)		10,096	4,302	10,096	4,302
Temp. (°C)	IN	34.93	25.87	34.93	25.87
	OUT	31.62	33.62	32.42	31.74
Q (kcal/h)		33,300		25,200	
Qavg (kcal/h)		29,250			

3.3 Performance analysis based on the number of total plates –

Fig. 4 shows the changes in the values of A and U when the number of plates was increased from 25 to 35 in the shell-plate-type heat exchanger with the same configuration as specified earlier; the general trend is that as the number of plates increases, the value of A increases, while the value of U decreases. Thus, with the same heat exchange rate, A and U values have an inversely proportional relationship to each other. We believe that the optimal number of plates is about 30, which is the point where A and U plots meet on the graph.



Effect of the number of plates on A and U



Effect of the number of plates on U*A and overdesign rate.

Furthermore, as shown in Fig. 5, when the number of plates increases, the U*A value and overdesign rate increase. This can be explained considering Eq. (4), in which case, when the number of plates is increased at a constant cold energy of 92,300 kcal/h, the effective area increases, thus, the effectiveness ϵ decreases, consequently leading to an

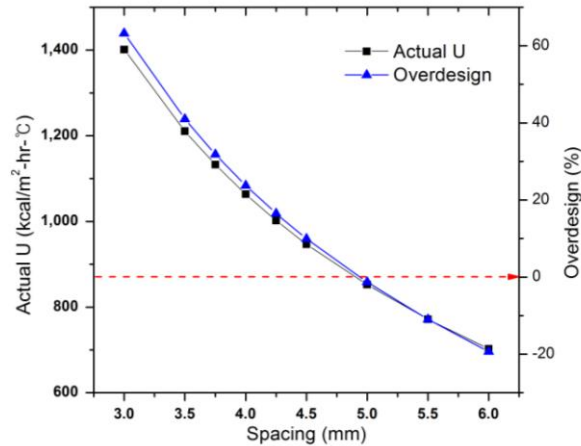
increase in the oversdesign rate. Because this system is free from fouling, the optimal value for the number of plates can be obtained where the oversdesign rate is zero; thus, based on Fig. 5, the optimal number of plates is about 29.

$$Q = \epsilon UA\Delta T \quad (4)$$

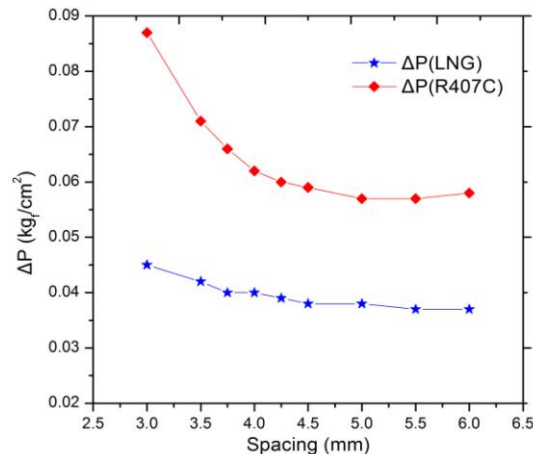
where ϵ indicates effectiveness. From the results of the two curves in Figs. 4 and 5, the optimal number of plates can be assumed to be 29–30.

3.4 Analysis based on the inter-plate spacing in the heat exchanger –

Figs. 6 and 7 show the changes in U and oversdesign rate and changes in pressure of the two liquids, respectively, when the spacing between plates of the heat exchanger is increased from 3 to 6 mm. As can be seen from Fig. 6, when the spacing between the plates increase, the U value and oversdesign rate show decreasing trends; assuming that the optimal value for plate spacing can be found when the oversdesign rate is zero, the optimal spacing between the plates is obtained as about 5.0 mm.



Effect of inter-plate spacing on U and oversdesign rate.



Effect of inter-plate spacing on fluid pressure.

From Fig. 7, it can be seen that, as the plate spacing in the shell-plate heat exchanger increases, the pressure differences of the fluids (ΔP) decrease as well; however, after about 4.0 mm, the pressure difference is almost constant. Further, because the pressure drop is less than 0.1 kgf/cm², it can be deduced that there is no effect of this pressure drop on the efficiency of the heat exchanger. Therefore, considering these results, it can be said that the optimal inter-plate spacing is 5.0 mm.

IV. CONCLUSIONS

We obtained the following results for our simulation study using the HTRI simulator for a shell-plate-type heat exchanger for a refrigeration warehouse that uses LNG cold energy with 27 plates having a 5-mm plate spacing, 0.4 T plate thickness, and effective area of 2.04 m² as reference values.

- (1) The simulation results for the primary heat exchanger yielded -121.5°C and -85°C for the LNG outlet temperature at the cold side and R407C outlet temperature at the hot side, which are considerably similar to the actual processing conditions at a refrigeration warehouse.
- (2) Because the heat exchange rates obtained from the water-water simulation of heat exchanger, i.e., Q_h , Q_c , and Q_{avg} of 33,300 kcal/h, 25,200 kcal/h, and 29,250 kcal/h, respectively, were similar to the experimental results, the reliability of the simulation results was ensured.
- (3) Under the same heat exchange rate, when the number of plates is increased, the $U \cdot A$ value increases, but because the ϵ value decreases, the oversize rate increases. Assuming that the optimal condition is obtained when the oversize rate is 0, the number of plates should be about 29–30.
- (4) It was observed that when the plate spacing of the heat exchanger increases, the U value and oversize rate of the heat exchanger decrease. The plate spacing with a 0% oversize rate is about 5.0 mm. In addition, when the plate spacing increases, the pressure difference decreases; however, after 4.0 mm, it is almost constant. Therefore, it can be concluded that the optimal inter-plate spacing is 5.0 mm.

V. POSTSCRIPT

This study was conducted as a project called: “Technology Development of Refrigeration Warehouse using LNG Cold Energy (-100°C or higher),” which was a part of the Energy Technology Development Program supported by the Korea Institute of Energy Technology Evaluation and Planning under the Ministry of Trade, Industry and Energy. We would like to express our sincere gratitude for KETEP support.

VI. REFERENCES

- [1] D.B. Han, Y.J. Kim, K.I. Yeom, J.R. Shin, Y.S. Baek “A study of simulation on the refrigerated warehouse system based on the cold energy of LNG using the Pro-II Simulator,” Korean Hydrogen and New Energy Society, vol. 28, no. 4, pp. 401-440, 2017.
- [2] H. Ryu, “Plate heat exchanger,” Korean Journal of Mechanical Science and Technology, vol. 35, no.9, pp.794-804.
- [3] P. Olaga, L. Leonid, O. Petro, L. Genadi, P. Anna, Y. Pavlo, “Two types of welded plate heat exchangers for efficient heat recovery in industry,” Applied Thermal Engineering, vol. 105, pp. 763-773, 2016.
- [4] M. Seo, Y. Kim, “Experimental study on heat transfer and pressure drop characteristics for single-phase flow in plate and shell heat exchangers,” Korean Journal of Air-Conditioning and Refrigeration Engineering, vol. 12, no. 4, pp. 422-429, 2000.
- [5] C.A. Bennett, R. S. Kistler, T. G. Lestina, “Improving heat exchanger designs,” Chemical Engineering Progress, vol. 103, pp. 40-45, 2007.
- [6] S. Jin, P. Hrnjak, “Effect of end plates on heat transfer of plate heat exchanger,” Journal of Heat and Mass Transfer, vol. 108, pp. 740-748, 2017.
- [7] S.W. Kim, C.H. Baek, K.S. Song, Y.C. Kim, “Condensation heat transfer and pressure drop of R245FA in a plate-shell heat exchanger,” Korean Journal of Air-Conditioning and Refrigeration Engineering, vol. 28, no. 12, pp. 495-501, 2016.